

Reflections on boosting wearable triboelectric nanogenerator performance via interface optimisation

Shravan Gokhool, Satyaranjan Bairagi, Charchit Kumar, Daniel M. Mulvihill*

Materials and Manufacturing Research Group, James Watt School of Engineering, University of Glasgow, Glasgow, G128QQ, UK

ARTICLE INFO

Keywords:

Textiles
Wearable electronics
Triboelectric nanogenerator
Surface modification
Plasma
Textile contact mechanics

ABSTRACT

An increasing need to harness power from our surroundings has led researchers to delve into the concept of green energy production from our environment. Textile and wearable triboelectric nanogenerators (t-TENGs or w-TENGs) are a promising option in this regard. Textile and wearable triboelectric nanogenerators can convert mechanical energy present in fabric movements into electrical power using modified textile materials or alternative base materials (such as polyester, PDMS, silicone, etc.). These devices are intended to be mounted on garments or directly on the skin making them highly portable, but could also be installed in any other areas where mechanical energy is present (shoes, floor, bag packs etc.). They have been proven to be capable of generating sufficient energy to power some low power devices and sensors. A key present limitation for textile TENGs is their low output compared to non-textile film based TENGs. In this review, we reflect on the task of boosting textile TENG performance via interface modification. Specifically, the paper surveys the improvements that have been possible via surface modification of textiles using different metals or metal oxides and plasma processes. Finally, some key areas are highlighted from a tribology and contact mechanics perspective that may have the potential to lead to further significant enhancements in performance; namely, designing fabric interfaces to boost contact area.

1. Introduction

Ever since its creation in the early 17th century, society has become even more reliant on electricity [1,2]. This phenomenon has caused our global annual power utilization to increase and 2019 research recorded an annual power utilization of up to an estimated 23,000 billion Watts per hour (or 23,000 TW/Hour) and that value is expected to grow within the coming years [3]. Various power generation options were created to meet these increasing annual demands which can range from environmentally friendly methods such as harnessing wind, solar or tidal power [4], to more harmful methods such as consuming fossil fuels, biomass or petroleum [5]. However, almost 64% of our overall global power is produced by fossil fuels (about 63.3%), whereas the rest of our power is produced using low carbon emission sources (nuclear, hydropower) and renewable methods (wind, solar, tidal) [6]. The overall concept of power consumption can be defined as the energy required to power large factories, cities, or even countries. This definition, known as mega energy, usually measures power consumption in giga Watts or mega Watts [7]. On the other hand, the concept of micro energy refers to the energy

consumed by smaller devices such as small electronic devices, smart devices and these only consume several milli-Watts to tens of Watts of power [8]. Although these devices consume small amounts of power, the number of individuals using those devices on a regular basis increases daily (over 3 billion today use some form of smart device), and thus a significant amount of total energy consumption is at play. Most smart and electronic devices rely on either disposable or rechargeable batteries. As devices improve and advance in functionality, their power consumption inevitably increases further. Therefore, batteries would need to consume and produce more power to meet the requirements of these devices which would make those devices bulkier and more inconvenient [8,9]. Furthermore, the increasing demand in power also puts a strain on global energy production [7] and our natural resources as most of our global power is produced by fossil fuels. The production, use, and disposal of batteries (lithium) in smart devices further adds a strain on both our global power production and environment [10]. This therefore leads to the pressing need for finding an alternative route to sustainable energy production [7]. Already existing energy harvesting alternatives heavily rely on their surrounding environments. For

* Corresponding author.

E-mail address: Daniel.Mulvihill@glasgow.ac.uk (D.M. Mulvihill).

<https://doi.org/10.1016/j.rineng.2022.100808>

Received 25 May 2022; Received in revised form 8 November 2022; Accepted 23 November 2022

Available online 30 November 2022

2590-1230/© 2022 The Authors. Published by Elsevier B.V. This is an open access article under the CC BY license (<http://creativecommons.org/licenses/by/4.0/>).

current at the low frequencies characteristic of normal human movement [25,26].

TENGs function through the combined effects of contact electrification and electrostatic induction. These are the main underlying phenomena enabling t-TENGs to convert mechanical energy into electrical energy [8,23,24]. t-TENGs are capable of converting mechanical energy into electrical current through the contact and separation (or indeed sliding) of two textile-based surfaces of dissimilar triboelectric polarity [27,28]. The triboelectric effect occurs during an induced electrification. This phenomenon is caused by the contact of a material (or textile surface) to another, which electrically charges both materials through contact or friction. Induced electrification occurs in all TENG devices when two dissimilar surfaces come into contact, forming a chemical bond between parts of the two surfaces (adhesion), leading to a charge transfer between both surfaces. Thus, electrons and ions will travel from the more negatively charged surface to the more positively charged surface to obtain an electrochemical equilibrium where both surfaces are equally charged and creating a neutral system. When separated, the charges from one of the surfaces are transferred to the other causing an unbalanced charged system. The opposite effect occurs when the surfaces re-enter into contact. The contact and separation induced triboelectric charges transferred from one surface to the other can generate a potential difference sufficient to create an AC current.

The underlying physics behind energy harvesting by the triboelectric effect was explained by Wang et al. [11]. This article explains, in detail, the relationship between TENG output and Maxwell's displacement current. According to Maxwell, the electric displacement vector is:

$$D = \epsilon_0 E + P \tag{1}$$

where, E is the electric field and P is the polarization vector. But in TENGs, where the displacement current is the crucial parameter influencing their output, a new term is introduced, and the displacement vector can be denoted as;

$$D = \epsilon_0 E + P + P_s \tag{2}$$

This is because, unlike in classic electromagnetic generators, the surface charges in nanogenerators are not induced by an external electric field. Therefore, the displacement current density of a TENG can be expressed as

$$JD = \frac{\partial D}{\partial t} + \frac{\partial P_s}{\partial t} \tag{3}$$

In TENGs, the determination of the current density depends mostly upon the surface charge density (σ_T) and dielectric constants (ϵ_1, ϵ_2) of the triboelectrification layers. Therefore, the current density at short circuit can be expressed as

$$JD \approx \sigma_T \frac{dH}{dt} \frac{\frac{d_1 \epsilon_0}{\epsilon_1} + \frac{d_2 \epsilon_0}{\epsilon_2}}{\left(\frac{d_1 \epsilon_0}{\epsilon_1} + \frac{d_2 \epsilon_0}{\epsilon_2} + z\right)^2} \tag{4}$$

The equation for output current from a TENG with an area A can be derived from Eq. (4) as

$$I \approx A \sigma_T \frac{dH}{dt} \frac{\frac{d_1 \epsilon_0}{\epsilon_1} + \frac{d_2 \epsilon_0}{\epsilon_2}}{\left(\frac{d_1 \epsilon_0}{\epsilon_1} + \frac{d_2 \epsilon_0}{\epsilon_2} + z\right)^2} \tag{5}$$

For a clearer understanding, Eq. (5) can be viewed as three separate parts. The first part, $P1$ denotes surface tribo-charge density (σ_T) which depends on the material properties of the contact pair. Whereas the second part $P2$ (dH/dt) is attributed to the mode of operation of the TENG of interest. The third part $P3$ explains the electrostatic induction aspect and illustrates how the charges induced on the back electrodes by the tribo-charges are governed by the permittivity of the material and the thicknesses of the layers [29].

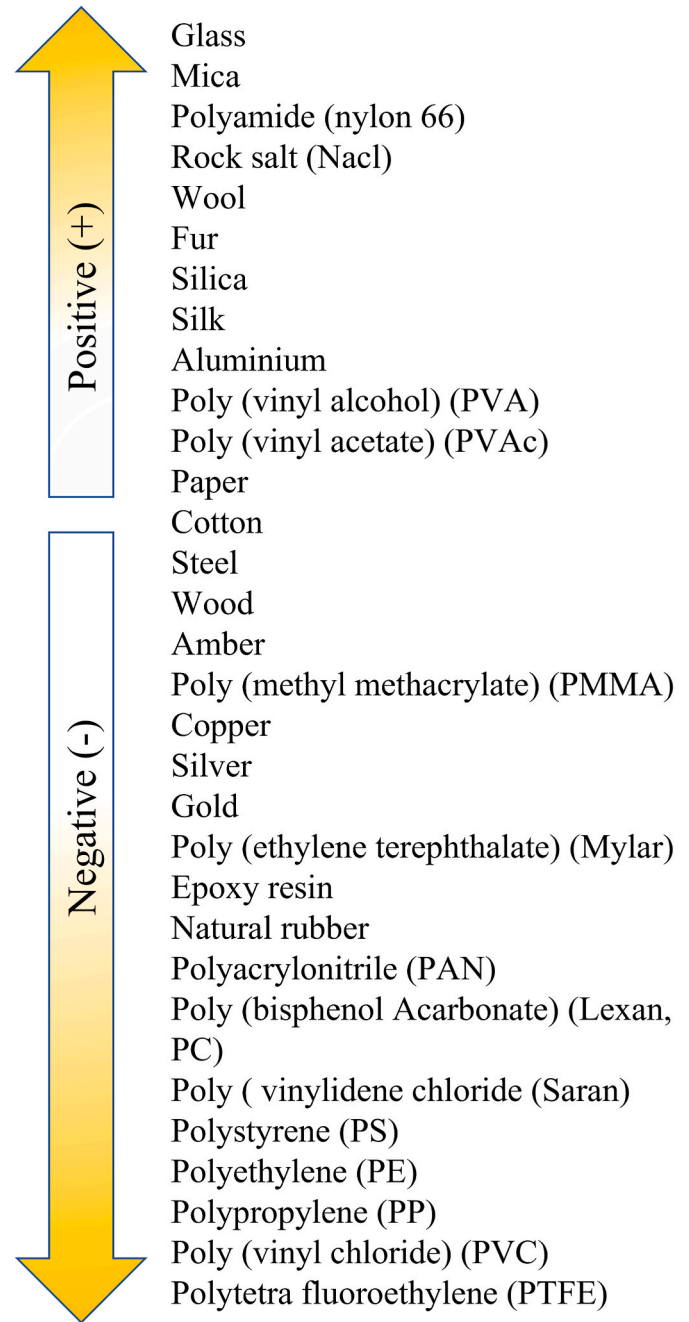


Fig. 2. Triboelectric series of materials [31].

$$P3 = \frac{\frac{d_1 \epsilon_0}{\epsilon_1} + \frac{d_2 \epsilon_0}{\epsilon_2}}{\left(\frac{d_1 \epsilon_0}{\epsilon_1} + \frac{d_2 \epsilon_0}{\epsilon_2} + z\right)^2} \tag{6}$$

From this equation, the effectiveness of a given TENG structure can be estimated.

A wide spectrum of materials display triboelectric properties, making several possible candidates for TENG applications. Additionally, the polarity, being either negative or positive, and charge density of the triboelectric materials are the key elements capable of dictating their ability to gain and/or lose electrons and can offer information on their interactions with different materials. The first triboelectric series was proposed and published in 1757 and was drafted by John Carl Wilcke [27,30]. The triboelectric series is a chart that classifies triboelectric materials based on their polarities and charge densities. Any materials

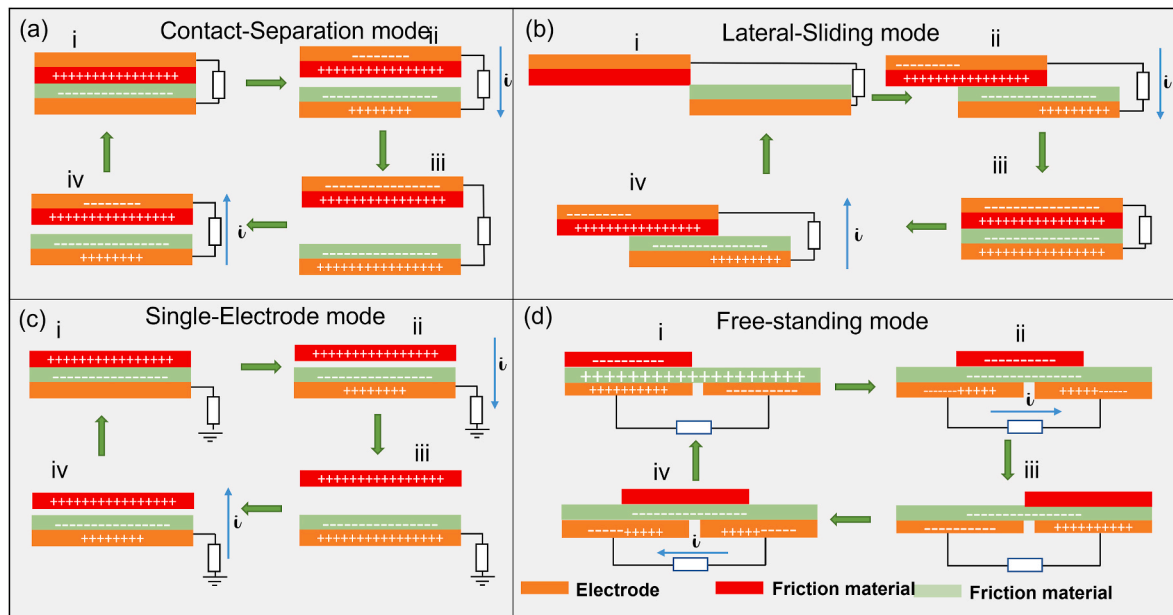


Fig. 3. Mode of operation for triboelectric nanogenerators (a) contact-separation mode, (b) lateral sliding mode, (c) single-electrode mode, and (d) freestanding triboelectric-layer mode [7].

that are listed further away from the middle of the chart are either more positively or negatively charged. The list below (Fig. 2) highlights some of the materials possessing triboelectric capabilities. A large number of pairings are possible, but in general, output is optimised by choosing materials with maximum separation on the triboelectric series.

There are four modes of operation of TENGs. Those modes were set out by the creator of the first set of devices, Wang et al. [32] who first proposed the four basic functioning modes in 2012. The schematic below (Fig. 3) offers an insight on how these devices function. Moreover, Fig. 3, offers information on how the concept of the triboelectric effect applies to various types of TENGs [7,33]. The four TENG functioning modes are described below:

(a) Vertical contact separation mode

This layout is probably the most commonly studied mode. Although simple, the underlying physics (i.e. triboelectrification and electrostatic induction) is clear. This mode involves the contact and separation of two dissimilar materials (Fig. 3a) in the normal direction only (i.e. without any sliding). As explained previously, the contact and separation of the surfaces leads to a charge transfer during contact and the repeated motion of these two dissimilar plates generates an AC current [8].

(b) Lateral sliding mode

This setup follows the same general principle as the vertical contact separation mode, but the movement is now lateral and gross sliding occurs between the surfaces. In this setup, the sliding movement of the two dissimilar dielectrics promotes current flow (Fig. 3b). In fact, the lateral sliding mode is capable of generating current through the creation of dissimilarly charged regions on both contacting surfaces of the device. As the two surfaces slide relative to one another, a potential build-up is caused in the non-overlapping parts on the electrode leading to a potential difference. An electron flow will therefore occur between the two electrodes. As the surfaces realign, the system reverts to a balanced state and regains its equilibrium. The sliding motion (in both directions) of the two plates can create an AC current flow [27,33].

(c) Single electrode mode

This device was created with the idea that one of the TENG layers would be capable of moving independently. As seen in Fig. 3c, the freely moving layer is not connected to an electrode. This layout is also known as the single electrode mode which is a dielectric to electrode (conductor) interaction. In this situation, the electrode acts as both the conductor of current and source of electrons [27].

(d) Freestanding triboelectric layer mode

This TENG uses two similarly laid out electrodes underneath a dielectric layer covering both electrodes. Fig. 3d highlights that the sliding motion of a top layer on the dielectric would create a current flow through the load resistance connected to the bottom electrodes.

3. Surface modification of textiles to enhance t-TENG performance

As mentioned in the introduction, various publications have strongly stressed the necessity to modify the surface of the textiles used to create t-TENG devices. Making the textile surfaces more tribopositive or tribonegative is one key aim and increasing the contact area between the devices is another [7]. Surface modification of the textile substrate can be done by different approaches such as chemical modification (mainly fluorinated or aminated based chemicals), 2D metals or metal oxide modification (Au, Ag, ZnO, TiO₂, CuO, etc), and plasma treatment (modification of the textile surface in the presence of argon, oxygen and fluoro based gases). This section is organised into two sub-sections; namely, surface modification via metals or metal oxides (Section 3.1) and modification of textiles using plasma processes (Section 3.2).

3.1. Surface modification of textiles via metals or metal oxides

This section will focus on wearable TENGs created using modified metals or metal oxides. The studies reviewed highlight devices created using a variety of metals paired with other polymers and materials (not solely metal oxides). Metal oxides are highly electropositive (see Fig. 2) and therefore, pairing them with nonferrous electronegative polymers offers the promise of increased output. This section also investigates the use of different structures which would alter the behaviours and applications of the devices.

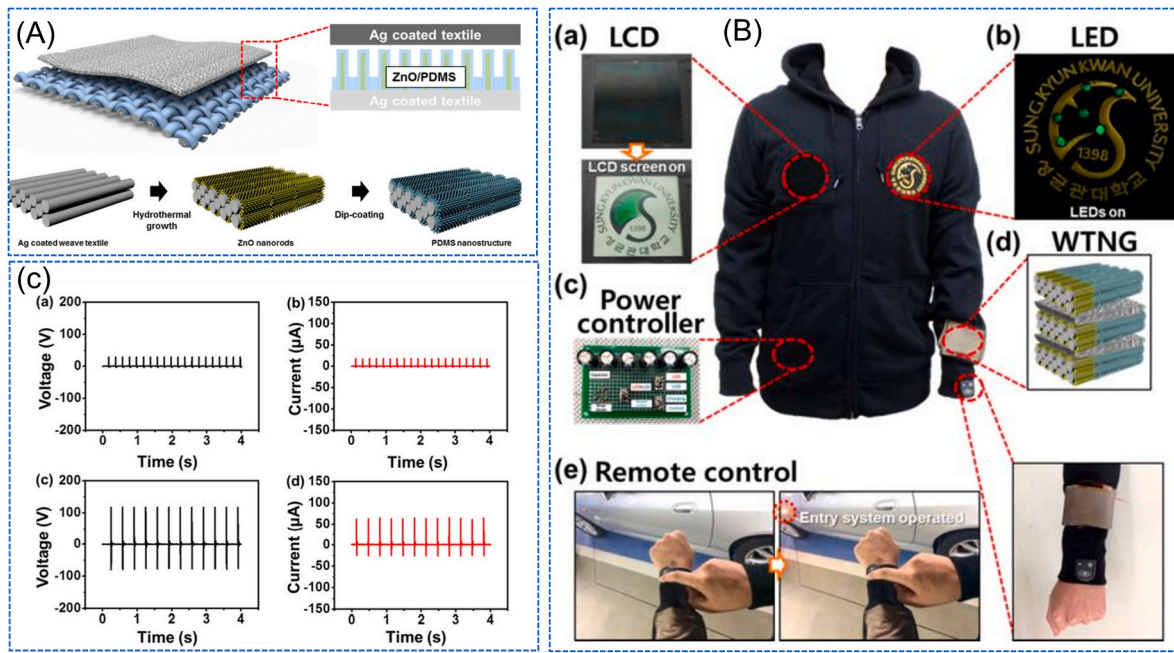


Fig. 4. A. Schematic diagram of the TENG and a flow diagram for PDMS nanopatterning, B. output voltage and current of the non-patterned PDMS (a & b) and patterned PDMS (c & d) based TENG, C. self-powering of LCD, LEDs and a remote-control unit using the wearable TENG [37].

In recent years, much research work on metals or metal oxide modified textiles for TENG devices have been reported. One such example, Bayan and colleagues [34] reported a textile based TENG composed of silver nanoparticles decorated with a graphitic carbon nitride ($g-C_3N_4$)/nylon layer on a conductive carbon cloth and commercial PTFE film. It was found that the silver-gCN/nylon based TENG exhibited better electrical performance (output voltage of ~ 200 V for silver-gCN/nylon while ~ 52 V for the CN modified TENG). This is because there is no charge migration between base carbon cloth and silver-gCN/nylon layer unlike base carbon cloth and CN layer. Also, the fabricated TENG could generate a maximum output current and power density of $\sim 1.1 \mu A$ and $\sim 3.1 \mu W/cm^2$, respectively. A study by

Salaudin et al. [35] have reported a laser carbonized M-Xene/ziolitic imidazolate 67 modified textile based TENG. Here, the developed TENG showed an output voltage of ~ 1340 V and power density of $\sim 65 W/m^2$, respectively. Yang and colleagues [36] reported a textile based TENG where graphene oxide (GO) incorporated PDMS modified conductive PET fabric was used as a negative tribo-layer and human skin as the positive tribo-layer. They found that, the fabricated TENG could generate an output voltage, current and power density of ~ 140.4 V, $\sim 2.57 \mu A$, and $\sim 37.29 mW/m^2$, respectively.

The next paper we look at by Seung et al. [37], delved into the development of a wearable TENG device capable of providing enough output to power small wearable devices such as keyless car remote

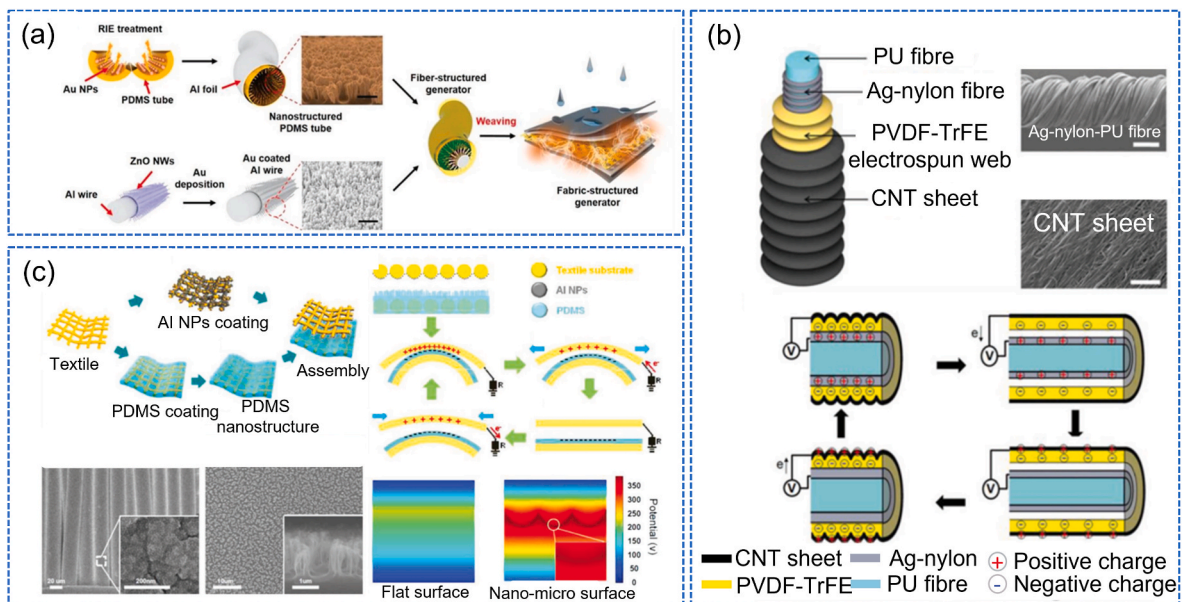


Fig. 5. (a) Flow diagrams of a textile based TENG based on a coaxial fibre (ZnO nanostructure modified Al wire in the core and PDMS in the shell) [38], (b) Schematic diagrams of a stretchable fibre based TENG device, and its working mechanism [39], and (c) Flow diagrams for a textile based TENG composed of PDMS modified Al NPs coated textile and its working mechanism [33].

controls and LED arrays as well as small LCD screens. Due to their availability, commercial metal-coated textile materials have been considered as forming a promising substrate for a wide range of wearable electronic devices and open up numerous applications due to their excellent mechanical strength, light weight, flexibility, and stretchability. Therefore, this research demonstrates a new type of fully flexible, foldable nanopatterned wearable TENG with a high power-generating performance and mechanical robustness. The devices created possessed a bottom layer comprised of an Ag-coated textile substrate with a PDMS nanopatterned ZnO nano-rod array template (Fig. 4A). The metal oxide nanorods were grafted onto the layers of the device through a hydrothermal process (which allows an evenly uniform coating of metal oxide nanorods on the surface of the textile) and measured between 100 nm and 1 μm . PDMS was applied to the textile surface through a dip-coating process. The top layer of the device only contained the Ag-coated textile substrate. It has been judged that the use of the PDMS and ZnO nanorods on the bottom layer would create a potential difference between the materials of the top layer, therefore creating current flow during contact and separation. Additionally, the charge transfer between the PDMS and Ag strongly depends on their position in the triboelectric series. In fact, due to their opposing charges on the triboelectric series (Ag being positively charged and PDMS negatively) the charges are capable of flowing from one surface to the other thus creating an alternative current flow. The research further highlighted the influence of nanopatterned PDMS in the device by comparing two devices: one device containing the nanopatterned PDMS and the other containing a smooth layer of PDMS. By testing both devices under identical conditions (same frequency and compressive force of 10 kgf) the output of the non-patterned PDMS was recorded to reach maximum output of 30 V and 20 μA whereas the nanopatterned PDMS was capable of outputting 120 V and 65 μA (Fig. 4B). Furthermore, this research showed the capability of creating a multi-layered vertical stacking which boosted the output of the device. A maximum output voltage of 170 V and a current of 120 μA were recorded. These output values equated to around 1.1 mW of power with a resistance of 1 M Ω . Even though multilayering led to a bulkier device, the power outputs on offer open up promising applications allowing it to be mounted in areas of the body with more room (such as under the soles of a shoe). This research was then further developed, and the device created was then implemented as the power source in a smart jacket containing an LED setup, an LCD screen and a keyless remote for a car (Fig. 4C).

In 2015, Kim et al. [38] explored the possibilities of using an alternative structure to create t-TENGs. This research focused on the use of a coaxial structure in which two dissimilar materials come into contact but separate from each other within the structure. Similar concepts have already been used in energy harvesting and storage devices in the form of other fibres such as solar panels, supercapacitors, and lithium-ion batteries. This structure offers a higher stability under bending and stretching to small movements. The device created as seen in Fig. 5a, consists of Al wires with vertically aligned nanowires and PDMS tubes with nanotextured surfaces (Fig. 5a). In this application, the Al wires would be used as a core while the PDMS tube is used as a shell (to completely seal the device). The Al wires contained ZnO nanoparticles grown through hydrothermal methods. Furthermore, an Au film was deposited on the inner surface of the tube to function as an electrode. This metal-based device measuring 5 cm in length and 6 mm in diameter, could then be implemented in various locations with enough space for a coaxial type of device. For example, such a structure could be implemented in shoes as they are capable of withstanding deformations and producing power under an alternating compressive load. It has been recorded that such devices can generate power outputs of 40 V and 10 μA with a 50 N load and 10 Hz excitation frequency [35].

Following the concept of using coaxial structures to create TENG devices, a paper by Sim et al. [39] focuses on a similar concept. In fact, they develop a fibre-based t-TENG with a coaxial structure possessing a wrinkle structure to increase its stretchability and power output.

Furthermore, this device can be applied to the body to utilise increased movements at fingers, elbows, and knee joints. As seen in Fig. 5b, the device is created using polyurethane (PU) fibres wrapped in nylon 66, yarns coated in silver (Ag) at 30 μm in diameter. The device also possesses a layer of polyvinylidene fluoride-co-trifluoro ethylene (PVDF-TrFE) – a highly tribo-negative material. The sample created has an average diameter of 440 μm , a resistance of 10.4 Ω in the initial state, and a length of 10 mm. As illustrated in Fig. 5b, the PU fibre acts as the core of the device while the overlapping layers generate electricity. In fact, the silver layer possesses a positive triboelectric charge whereas the PVDF-TrFE acts as a highly tribo-negative material. The vertical sliding and contact separation of both layers would promote flow of electrons between both layers. Finally, a layer of CNTs was applied on the outer part of the device to act as an electrode. It has been shown that using a wrinkle structure would better improve current outputs from the device. The authors confirm this by stating that the wrinkle structure is capable of being more stretchable and therefore can promote more contact between the surfaces of the device.

A paper by Lee et al. [40] focused on increasing the triboelectric output of devices using nanostructures on the surface of the device's contacting layers. The device was created using Al nanostructures and nanostructured PDMS as triboelectric materials with super flexible Au-coated fabrics. It has been recorded that paring metal and metal oxide layers with polymers can increase the number of charges being transferred from layer to layer as these materials are widely separated on the triboelectric series. Fig. 5c indicates how the device was created. As seen in the figure, the top textile yarns were coated with Al NP (aluminium nanoparticles) through thermal evaporation at room temperature with a deposition rate of 0.2 \AA^{-1} , a deposition thickness of 4 nm and pressure of 10–7 Torr. The bottom textile yarns were covered with a PDMS layer through spin-coating at a rate of 200 rpm for 60 s and were then cured at 60 $^{\circ}\text{C}$ for 4 h. The nanostructured patterns (all uniformly distributed over the surface each possessing a diameter of 150 nm and 2.5 μm in height) were then achieved through a RIE plasma process in which a radio wave frequency of 100 W was applied for 20 min in a chamber filled with a mixed gas with 13 sccm of O_2 and 37 sccm of CF_4 . The obtained nanostructured configurations with a diameter of about 150 nm and a length of 2.5 μm were uniformly distributed onto the surface of the PDMS. Both layers created were then laid facing each other for voltage and current tests. These tests involved performing contact and separation of both layers at different pressure and frequency values. The nanostructured surfaces were also compared with flat surfaces created using the same materials and process. It was noted that the electrical surface potential of the nanostructured surface was around 1.8 times higher than that of the flat surface. The result highlighted that the nanostructured surface had an electrical surface potential of 383 V. Further theoretical calculation confirmed that increasing the roughness of the surface could indeed increase the electrical potential of the device, thus increasing power output. To demonstrate the capabilities of the device, a signal analyser was used to measure both voltage and current outputs. The device measured 7 \times 7 cm^2 . The device was repetitively compressed and released at bending length of 3 cm and speed of 20 mm s^{-1} while V_{oc} and I_{sc} for the devices were measured at a resistance of $10^5 \Omega$. The fabric with nanostructured Al NPs generated a maximum output voltage of 259 V and output current of 78 μA . The devices output power density has been recorded as 33.6 mW/cm^2 .

To summarise, the papers studied above highlight the capabilities of using metal sheets and metal oxide depositions to further promote t-TENG power outputs. The research also highlights the importance of paring metals and metal oxides with tribo-negative polymers and various composites to obtain a better transfer of electrons from surface to surface thus facilitating better output performance.

3.2. Modification of textiles using plasma processes

We have seen that selection of TENG tribo-materials that are widely

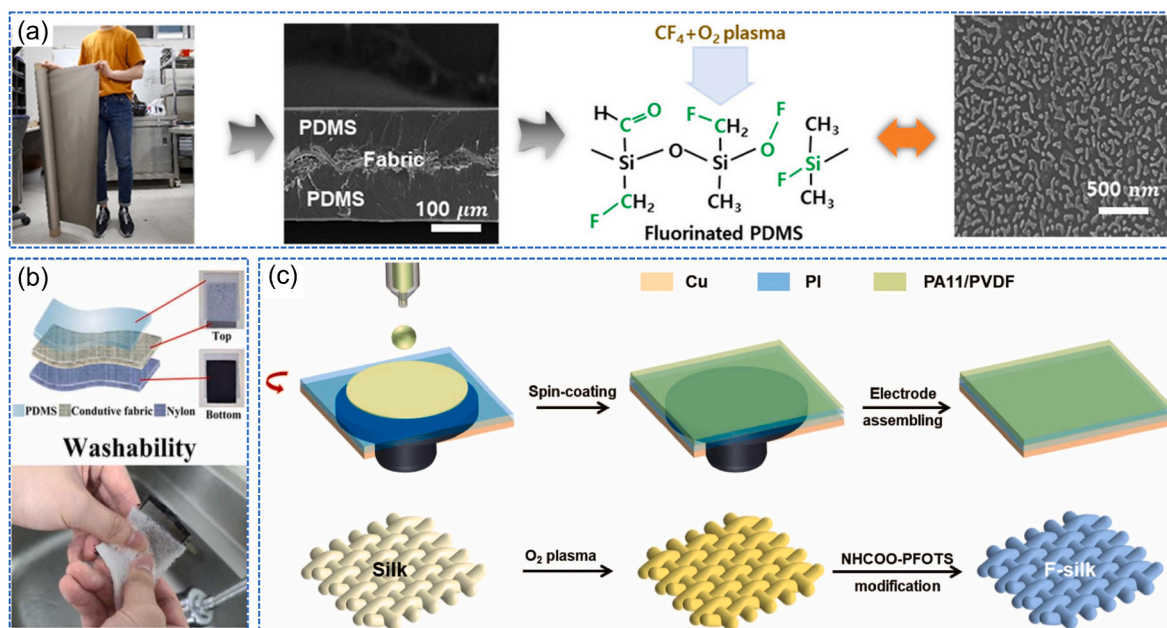


Fig. 6. (a) Textile TENG based on plasma treated PDMS-Ni-Cu textile [42], (b) Textile TENG based on plasma treated PDMS-nylon fabric [36], and (c) process flowchart for a textile TENG based on plasma and NHCOO-PFOT treated silk woven fabric [43].

spaced on the triboelectric series is an obvious starting point in TENG design (e.g. metal oxides and polymers). However, boosting contact area and modifying the chemical characteristics of triboelectric materials are also routes that can be used to enhance TENG performance. In this regard, plasma treatment is one of the promising strategies to enhance output response of textile based TENGs. Textile samples can be modified by the plasma process with various chemical environments such as argon (Ar), oxygen (O₂) and fluorocarbon (CF₄) based gases, etc [41].

A number of interesting recent contributions have been made in the area of plasma treated textile based TENGs. For example, Lee and colleagues [42] reported a textile TENG based on chemical surface engineered PDMS by plasma treatment (Fig. 6a). For preparation of the chemically surface engineered PDMS layer, first a Ni-Cu textile was dipped in a PDMS solution made from 10:1 ratio of the PDMS polymer and its curing agent followed by curing at 90 °C for 2 h. Thereafter, PDMS coated Ni-Cu textile was processed by a two-step plasma process. In the first step, the PDMS modified textile was treated by Ar gas plasma at 20 W radio frequency for 10 min at the gas pressure of 10 mTorr. Then, in the next step, the Ar treated PDMS layer was treated against CF₄ and O₂ plasma, respectively at a flow rate of 30 sccm and 10 sccm. After completing this plasma process, triboelectric performances were measured against an Al metal layer and it was found that the developed textile TENG device could generate output voltage and current of 110 V and 11.5 μA, respectively. The t-TENG device was able to generate a maximum power density of 13.3 W/m² with plasma exposure time of 2 min. The output response of the two-step plasma treated PDMS based device is higher compared to 1-step plasma treated PDMS (2.5 V output voltage and 0.25 μA current) and also higher than the reference case without plasma treated PDMS (output voltage of 62.5 V and output current of 6.31 μA). The 1-step Ar plasma treated PDMS based device showed lower output response even as compared to the reference untreated PDMS based TENG device - this may be because the oxidation of the PDMS layer causes lower affinity to attract or donate electrons to the Al layer.

Similarly, a textile based TENG was developed via SF₆ plasma treated PDMS layer (Fig. 6b) by Yang et al. [36]. In this study, the authors prepared different types of PDMS layers such as flat PDMS, rough PDMS, porous PDMS, and GO incorporated porous PDMS, to observe their effect in triboelectric response against human skin. Interestingly, it was found

that the GO with porous PDMS layer based TENG showed higher output voltage, current and power of 79.47 V, 2.43 μA, and 130.5 μW at the frequency of 4 Hz and 4 N applied force, respectively, compared to the other PDMS layer based TENGs. According to the authors, one explanation is that the porous PDMS layer has higher surface roughness compared to flat PDMS and may generate increased contact area between human skin and the PDMS layer under applied pressure. Besides the porous structure, GO also has different functional groups like C-O, C=O, C=C-C, which can make hydrogen bonds in the presence of an aqueous medium and therefore, the PDMS porous surface gets modified by GO. In addition, the GO modified porous PDMS layer showed higher surface electronegativity which causes higher triboelectric responses as compared to other PDMS layers. Therefore, it can be concluded from the above two studies that an additional metal oxide filler based PDMS layer along with plasma treatment against Ar, O₂ or any fluorine-based gases could be a good choice to develop more optimised textile based TENGs.

Likewise, in another study, Feng and co-workers [44] developed a textile fabric based TENG, where plasma and chemically treated polyester velvet fabric and PTFE were used as the positive and negative triboelectric layers, respectively. The polyester velvet fabric was first treated with O₂ plasma and then the plasma treated fabric was immersed into the acylated CNTs solution followed by ultrasonication for 20 min at 50 °C. Thereafter, the CNT treated fabric was immersed into a 0.2 wt% poly (ethylenimine) (PEI) solution at 40 °C for 20 min. Finally, the developed fabric was characterized by different techniques, and it was found that the textile TENG device made from CNT/PEI treated velvet fabric and PTFE, can generate output voltage and current of 56.4 V and 6.51 μA, respectively. The same research group has also developed a wearable, machine washable and self-cleanable textile fabric based triboelectric energy harvester (Fig. 6c) [43]. Herein, urethane perfluorooctyl silane (NHCOO-PFOT) modified silk woven fabric and spin coated polyamide 11 (nylon 11) were used as the triboelectric layers. Before modification of the silk fabric, oxygen plasma was carried out to break -OH groups in silk fabric so that NHCOO-PFOT can form covalent bonds with the silk fabric. The developed textile based TENG (fluorine modified silk and nylon 11) has shown 465.63 V output voltage and 26.04 μA current, respectively at 6 N applied load and 5 Hz frequency, which is higher as compared to the bare silk fabric and nylon 11 fabric

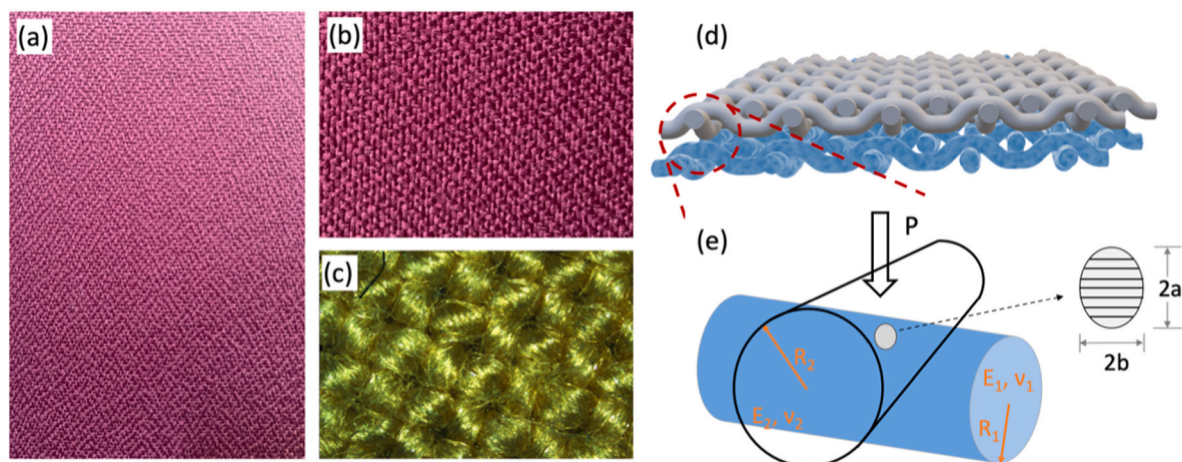


Fig. 7. (a) Photograph of fibre-based woven textile cloth, (b) Magnified view of figure a, (c) Optical image of the textile surface, (d) 3D drawing of the two textile substrates, (e) Inset illustrating the small contact area developed at textile-textile interfaces with yarn or fibre contact idealised as the contact between two cylinders of radius R_1 and R_2 . P is the applied load (at a single contact spot), $2a$ and $2b$ define the dimensions of the tiny contact ellipse and E and ν represent Young's modulus and Poisson's ratio.

based TENG (185.41 V and 9.55 μ A). The reason for the improvement is the raised electron affinity of the silk fabric in the presence of NHCOO-PFOT compared to pristine silk fabric. The developed t-TENG gave a maximum power density of 2.08 W/m² at an external load of 10 M Ω . Therefore, it can be concluded from these studies that florin-based treatment is more suitable to obtain better triboelectric effect from textile based TENGs compared to amine or other treatments.

4. Limitations and opportunities in the tribology and contact of textiles

In general, as we have seen above, much of the research carried out has been in the direction of employing surface modification or chemical treatments at a global scale over the whole fabric surface. However, a crucial interfacial aspect governing the output of textile TENGs has received very little attention: that of the contact area produced in textile TENGs and its governing contact mechanics at different length scales. A recent work by Min et al. [45] showed how electrical output is highly sensitive to real contact area. This makes sense, because electrons rely on true contact in order to transfer from one surface to another – thus, higher contact area produces greater electrical output. In turn, as is well accepted in the tribology literature, contact area grows as the force pressing the surfaces together increases. The work by Min et al. was on conventional non-textile TENGs, but the key link between contact area and electrical output will also apply to textile TENGs. In fact, low levels of contact between textile fabrics may be the reason why textile TENG output lags significantly behind that of non-textile film-based TENGs. Indeed, contact area is likely to be particularly small at low contact pressures – exactly the case pertaining in the case of wearable textiles! If one looks at textile contact at the local scale, the contact formation between two yarns (and between two fibres) can be simplified essentially as that of contact between two cylinders (Fig. 7). The contact formed between two contacting bodies is mutually determined by both materials' mechanical properties, shape, chemical characteristics, and surface roughness. Knowing the Young's moduli (E_1 and E_2), Poisson's ratio's (ν_1 and ν_2) and geometric parameters (radius and length), one can estimate the contact size assuming a simple Hertz calculation. Given that the diameters of textile fibres are of the order of tens of microns, the contact area developed between the cylinders will be tiny as illustrated in Fig. 7. A textile-textile interface will clearly consist of several discrete fibre contacts, but even so, the resulting total area will still be a small fraction of the nominal area. With recent advancements in *in-situ* real contact visualization techniques, it has become possible to precisely

record the distribution of real contact regions during contact formation for solid-solid interfaces [46–48]. However, considering the ultra-small length scale of the contact patches and high complexity of the textile system, the exact measurement of real contact area and localized contact stresses appears a challenging task. Moreover, localized interactions between yarns take place at sub-microscopic scale, therefore this would require a dedicated high-resolution tool for real contact area characterisation. One of the key aspects limiting textile TENG output is likely to be this low contact area and boosting it is a task worthy of considerable attention. Advancements in characterising the contact area could assist us in modifying existing weaving techniques to develop multi-directional textiles at multi-dimensional levels. Development of specific shaped nano-scale structures on two interacting woven fabrics (working as two tribo-layers at the local scale) could increase the effective real contact area. Likewise, fabric structures that minimise the gaps between fibres (i.e. via branching nano fibres) are also likely to boost contact area; thereby, boosting textile TENG output. Some progress has already been made in this direction by using electrospinning to create a greater density of fibre contacts [49–59]. A comprehensive review of electrospun nanofibre based TENGs for wearable applications is given in Babu et al. [59]. This kind of work is vastly under-developed, and much progress remains to be made.

5. Conclusions

With the advancement of electronic technology, demand for wearable and portable electronic gadgets is gradually increasing in the global market. Therefore, provision of a sustainable source of power for these devices has become an important topic. In the wearables industry, battery packs are still widely used due to the importance of guaranteeing a reliable power supply and also owing to the underdeveloped state of play with wearable energy harvester technology. One of the most promising energy harvesting solutions for wearables is the textile triboelectric nanogenerator. However, textile TENG output remains considerably lower than that of non-textile conventional TENGs. There are likely to be two main reasons for this: (1) surface modification is more difficult and less advanced on textiles and (2), the contact area developed at textile-textile interfaces is small. In this review, we reflected on some of the approaches that can be deployed to boost wearable TENG output particularly with regard to the interface. Specifically, we showed how surface modification of textiles either by chemicals or plasma treatment has shown promise. Surface modification by different means such as metal or metal oxides and plasma treatment have been

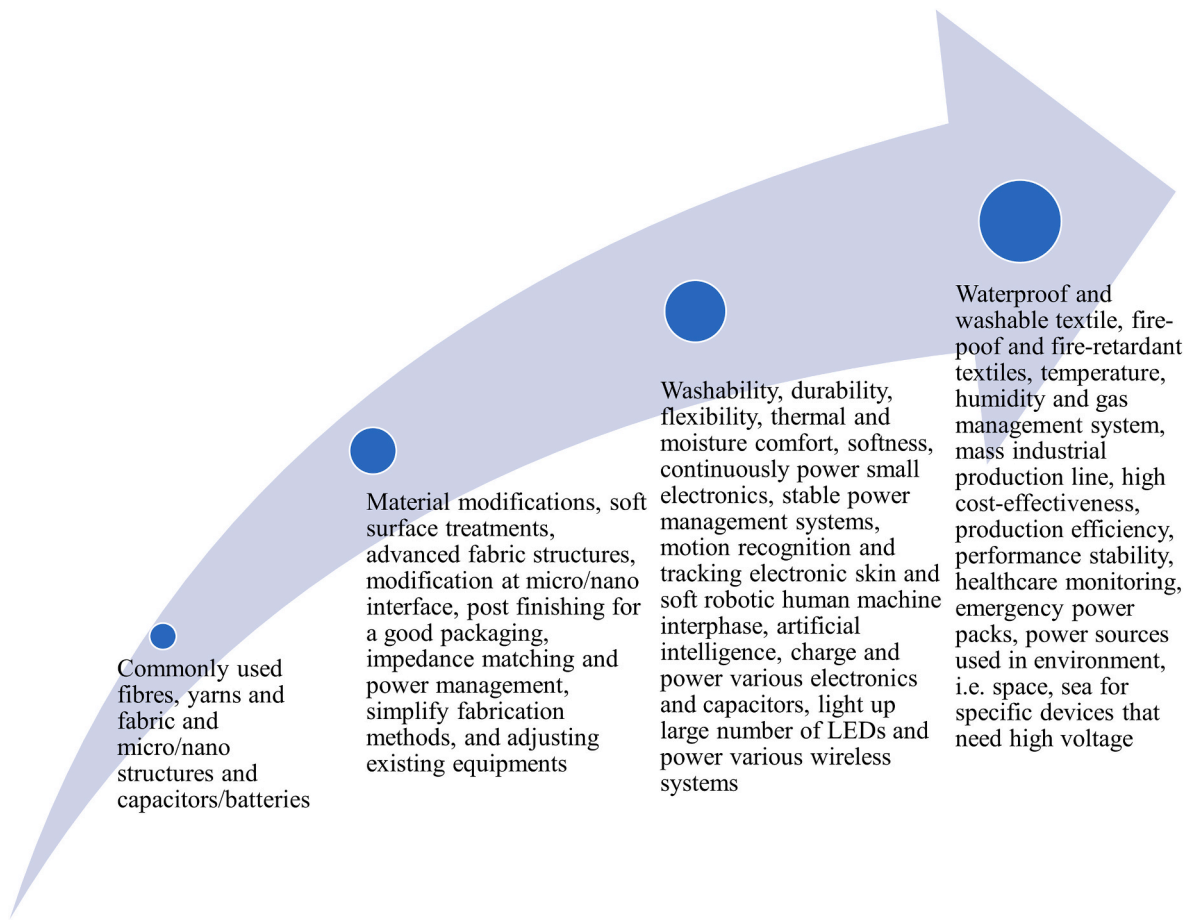


Fig. 8. Road map indicating future trends in the development of textile-based TENG technology [60].

found to produce modest improvements in output. However, considerable further improvement is required before textile TENGs are in a position to match the performance of conventional film based TENGs. By reflecting on the underpinning tribology and mechanics of textile contact, we have highlighted one important challenge that has the potential to produce significant further gains: that of boosting contact area in textile TENGs by introduction of novel fibre structures perhaps at smaller and smaller scales to reduce the occurrence of gaps that prevent charge transfer. If significant gains can be made in output performance, the application potential for textile TENGs in the wearable electronics sector is enormous. The textile based TENG is best utilized for small-scale electronics which require very small amounts of power. Low power wearable sensors and devices are prime examples. TENG potential is much less clear for larger scale power requirements. A road map indicating future trends in textile based TENG technology is shown in Fig. 8 [60].

Credit author statement

Shravan Gokhool: Conceptualization, Investigation, Methodology, Software, Writing – original draft, Writing – review & editing; Satyranjan Bairagi: Conceptualization, Investigation, Methodology, Software, Writing – original draft, Writing – review & editing; Charchit Kumar: Conceptualization, Investigation, Methodology, Software, Writing – original draft, Writing – review & editing; Daniel M. Mulvihill: Lead Supervision, Conceptualization, Resources, Writing – original draft, Writing – review & editing, Project administration, Funding acquisition.

Declaration of competing interest

The authors declare that they have no known competing financial interests or personal relationships that could have appeared to influence the work reported in this paper.

Data availability

Data will be made available on request.

Acknowledgements

The authors acknowledge the support of the UK Engineering and Physical Sciences Research Council (EPSRC) for funding and supporting the work through grant Ref. EP/V003380/1 ('Next Generation Energy Autonomous Textile Fabrics based on Triboelectric Nanogenerators').

References

- [1] World Energy Statistics | Energy Supply & Demand | Enerdata, (n.d.). https://www.enerdata.net/publications/world-energy-statistics-supply-and-demand.html?gclid=Cj0KCQjw06OTBhC_ARIsAAU1yOWDkkSjPte26ffQmIZwr82InO-SSXEtL5iTOv8WRpddkxQDpFM6f40aAtXhEALw_wcB (accessed April 27, 2022).
- [2] A.K. Erenoğlu, O. Erdiñç, A. Taşcıkaraoğlu, *History of Electricity, Pathways to a Smarter Power Syst*, 2019, pp. 1–27.
- [3] • Global Electricity Consumption by Country 2020 | Statista, (n.d.). <https://www.statista.com/statistics/267081/electricity-consumption-in-selected-countries-worldwide/> (accessed April 27, 2022).
- [4] P.A. Owusu, S. Asumadu-Sarkodie, A review of renewable energy sources, sustainability issues and climate change mitigation, *Cogent Eng* 3 (2016), <https://doi.org/10.1080/23311916.2016.1167990>.
- [5] M.A. Rosen, *Renewable Energy and Energy Sustainability*, INC, 2021, <https://doi.org/10.1016/B978-0-12-821602-6.00002-X>.

- [6] M.R. Ritchie, Hannah, *Energy. Our World in Data*, 2020.
- [7] C. Zhang, Z.L. Wang, *Triboelectric Nanogenerators* (2018), https://doi.org/10.1007/978-981-10-5945-2_38.
- [8] S.S. Kwak, H.J. Yoon, S.W. Kim, Textile-based triboelectric nanogenerators for self-powered wearable electronics, *Adv. Funct. Mater.* 29 (2019) 1–26, <https://doi.org/10.1002/adfm.201804533>.
- [9] J. Zhong, Y. Zhang, Q. Zhong, Q. Hu, B. Hu, Z.L. Wang, J. Zhou, Fiber-based generator for wearable electronics and mobile medication, *ACS Nano* 8 (2014) 6273–6280, <https://doi.org/10.1021/nn501732z>.
- [10] J. Luo, W. Gao, Z.L. Wang, The triboelectric nanogenerator as an innovative technology toward intelligent sports, *Adv. Mater.* (2021), <https://doi.org/10.1002/adma.202004178>.
- [11] Z.L. Wang, On Maxwell's displacement current for energy and sensors: the origin of nanogenerators, *Mater. Today* 20 (2017) 74–82, <https://doi.org/10.1016/j.mattod.2016.12.001>.
- [12] K. Xia, Z. Zhu, H. Zhang, Z. Xu, A triboelectric nanogenerator as self-powered temperature sensor based on PVDF and PTFE, *Appl. Phys. Mater. Sci. Process* 124 (2018) 1–7, <https://doi.org/10.1007/s00339-018-1942-5>.
- [13] Z. Wen, M.-H. Yeh, H. Guo, J. Wang, Y. Zi, W. Xu, J. Deng, L. Zhu, X. Wang, C. Hu, L. Zhu, X. Sun, Z.L. Wang, Self-powered textile for wearable electronics by hybridizing fiber-shaped nanogenerators, solar cells, and supercapacitors, *Sci. Adv.* 2 (2016), e1600097, <https://doi.org/10.1126/sciadv.1600097>.
- [14] Z. Li, Q. Zheng, Z.L. Wang, Z. Li, Nanogenerator-based self-powered sensors for wearable and implantable electronics, *Research* 2020 (2020) 1–25, <https://doi.org/10.34133/2020/8710686>.
- [15] C. Chen, L. Chen, Z. Wu, H. Guo, W. Yu, Z. Du, Z.L. Wang, 3D double-faced interlock fabric triboelectric nanogenerator for bio-motion energy harvesting and as self-powered stretching and 3D tactile sensors, *Mater. Today* 32 (2020) 84–93, <https://doi.org/10.1016/j.mattod.2019.10.025>.
- [16] Y. Han, F. Yi, C. Jiang, K. Dai, Y. Xu, X. Wang, Z. You, Self-powered gait pattern-based identity recognition by a soft and stretchable triboelectric band, *Nano Energy* 56 (2019) 516–523, <https://doi.org/10.1016/j.nanoen.2018.11.078>.
- [17] X. Peng, K. Dong, C. Ye, Y. Jiang, S. Zhai, R. Cheng, D. Liu, X. Gao, J. Wang, Z. L. Wang, A breathable, biodegradable, antibacterial, and self-powered electronic skin based on all-nanofiber triboelectric nanogenerators, *Sci. Adv.* 6 (2020), <https://doi.org/10.1126/sciadv.aba9624>.
- [18] W. Gao, S. Emaminejad, H.Y.Y. Nyein, S. Challa, K. Chen, A. Peck, H.M. Fahad, H. Ota, H. Shiraki, D. Kiriya, D.H. Lien, G.A. Brooks, R.W. Davis, A. Javey, Fully integrated wearable sensor arrays for multiplexed in situ perspiration analysis, *Nature* 529 (2016) 509–514, <https://doi.org/10.1038/nature16521>.
- [19] W. Sun, B. Li, F. Zhang, C. Fang, Y. Lu, X. Gao, C. Cao, G. Chen, C. Zhang, Z. L. Wang, Teng-Bot, Triboelectric nanogenerator powered soft robot made of unidirectional dielectric elastomer, *Nano Energy* 85 (2021), <https://doi.org/10.1016/j.nanoen.2021.106012>.
- [20] S. Hao, J. Jiao, Y. Chen, Z.L. Wang, X. Cao, Natural wood-based triboelectric nanogenerator as self-powered sensing for smart homes and floors, *Nano Energy* 75 (2020), 104957, <https://doi.org/10.1016/j.nanoen.2020.104957>.
- [21] X. Xue, P. Deng, B. He, Y. Nie, L. Xing, Y. Zhang, Z.L. Wang, Flexible self-charging power cell for one-step energy conversion and storage, *Adv. Energy Mater.* 4 (2014) 1–5, <https://doi.org/10.1002/aenm.201301329>.
- [22] T.E. Starner, J.A. Paradiso, Human-generated power for mobile electronics, *Low-Power Electron. Des.* 1990 (2004) 1–45, <https://doi.org/10.1201/9781420039559.ch45>.
- [23] M.J. Datta, M.N. Horenstein, The electrostatics of charged insulating sheets peeled from grounded conductors, *J. Phys. Conf. Ser.* 142 (2008), 012076, <https://doi.org/10.1088/1742-6596/142/1/012076>.
- [24] A.F. Diaz, R.M. Felix-Navarro, A semi-quantitative tribo-electric series for polymeric materials: the influence of chemical structure and properties, *J. Electrostat.* 62 (2004) 277–290, <https://doi.org/10.1016/j.elstat.2004.05.005>.
- [25] A. Chen, C. Zhang, G. Zhu, Z.L. Wang, Polymer materials for high-performance triboelectric nanogenerators, *Adv. Sci.* 7 (2020) 1–25, <https://doi.org/10.1002/advs.202000186>.
- [26] H. Zou, L. Guo, H. Xue, Y. Zhang, X. Shen, X. Liu, P. Wang, X. He, G. Dai, P. Jiang, H. Zheng, B. Zhang, C. Xu, Z.L. Wang, Quantifying and understanding the triboelectric series of inorganic non-metallic materials, *Nat. Commun.* 11 (2020) 1–7, <https://doi.org/10.1038/s41467-020-15926-1>.
- [27] S. Wang, L. Lin, Z.L. Wang, Triboelectric nanogenerators as self-powered active sensors, *Nano Energy* 11 (2015) 436–462, <https://doi.org/10.1016/j.nanoen.2014.10.034>.
- [28] H. Zou, Y. Zhang, L. Guo, P. Wang, X. He, G. Dai, H. Zheng, C. Chen, A.C. Wang, C. Xu, Z.L. Wang, Quantifying the triboelectric series, *Nat. Commun.* 10 (2019) 1–10, <https://doi.org/10.1038/s41467-019-09461-x>.
- [29] R. Zhang, H. Olin, *Material choices for triboelectric nanogenerators: a critical review*, *EcoMat* 2 (2020), e12062.
- [30] K. Dong, Z.L. Wang, Self-charging power textiles integrating energy harvesting triboelectric nanogenerators with energy storage batteries/supercapacitors, *J. Semiconduct.* 42 (2021), <https://doi.org/10.1088/1674-4926/42/10/101601>.
- [31] S. Liu, T. Hua, X. Luo, N. yi Lam, X. ming Tao, L. Li, A novel approach to improving the quality of chitosan blended yarns using static theory, *Textil. Res. J.* 85 (2015) 1022–1034, <https://doi.org/10.1177/0040517514559576>.
- [32] Y. Zi, Z.L. Wang, Nanogenerators: an emerging technology towards nanoenergy, *Apl. Mater.* 5 (2017), <https://doi.org/10.1063/1.4977208>.
- [33] W. Paosangthong, R. Torah, S. Beeby, Recent progress on textile-based triboelectric nanogenerators, *Nano Energy* 55 (2019) 401–423, <https://doi.org/10.1016/j.nanoen.2018.10.036>.
- [34] S. Bayan, S. Pal, S.K. Ray, Interface engineered silver nanoparticles decorated g-C₃N₄ nanosheets for textile based triboelectric nanogenerators as wearable power sources, *Nano Energy* 94 (2022), <https://doi.org/10.1016/j.nanoen.2022.106928>, 106928.
- [35] M. Salauddin, S.S. Rana, M. Sharifuzzaman, S.H. Lee, M.A. Zahed, Y. Do Shin, S. Seonu, H.S. Song, T. Bhatta, J.Y. Park, Laser-carbonized MXene/ZiF-67 nanocomposite as an intermediate layer for boosting the output performance of fabric-based triboelectric nanogenerator, *Nano Energy* 100 (2022), 107462, <https://doi.org/10.1016/j.nanoen.2022.107462>.
- [36] H.J. Yang, C.T. Ko, S.F. Chang, M.J. Huang, Study on fabric-based triboelectric nanogenerator using graphene oxide/porous PDMS as a compound friction layer, *Nano Energy* 92 (2022), 106791, <https://doi.org/10.1016/j.nanoen.2021.106791>.
- [37] W. Seung, M.K. Gupta, K.Y. Lee, K. Shin, J. Lee, T.Y. Kim, S. Kim, J. Lin, J.H. Kim, S. Kim, *Nanopatterned Textile-Based*, 2015, pp. 3501–3509.
- [38] K.N. Kim, J. Chun, J.W. Kim, K.Y. Lee, J.U. Park, S.W. Kim, Z.L. Wang, J.M. Baik, Highly stretchable 2D fabrics for wearable triboelectric nanogenerator under harsh environments, *ACS Nano* 9 (2015) 6394–6400, <https://doi.org/10.1021/acsnano.5b02010>.
- [39] H.J. Sim, C. Choi, S.H. Kim, K.M. Kim, C.J. Lee, Y.T. Kim, X. Lepró, R. H. Baughman, S.J. Kim, Stretchable triboelectric fiber for self-powered kinematic sensing textile, *Sci. Rep.* 6 (2016) 1–7, <https://doi.org/10.1038/srep35153>.
- [40] S. Lee, W. Ko, Y. Oh, J. Lee, G. Baek, Y. Lee, J. Sohn, S. Cha, J. Kim, J. Park, J. Hong, Triboelectric energy harvester based on wearable textile platforms employing various surface morphologies, *Nano Energy* 12 (2015) 410–418, <https://doi.org/10.1016/j.nanoen.2015.01.009>.
- [41] H.-S.Z. Peng Huang, Dan-Liang Wen, Yu Qiu, Ming-Hong Yang, Tu Cheng, X. S. Zhang, *Textile-based triboelectric nanogenerators for wearable*, *Micromachines* 12 (2021) 1–21.
- [42] C. Lee, S. Yang, D. Choi, W. Kim, J. Kim, J. Hong, Chemically surface-engineered polydimethylsiloxane layer via plasma treatment for advancing textile-based triboelectric nanogenerators, *Nano Energy* 57 (2019) 353–362, <https://doi.org/10.1016/j.nanoen.2018.12.051>.
- [43] M. Feng, Y. Wu, Y. Feng, Y. Dong, Y. Liu, J. Peng, N. Wang, S. Xu, D. Wang, Highly wearable, machine-washable, and self-cleaning fabric-based triboelectric nanogenerator for wireless drowning sensors, *Nano Energy* 93 (2022), 106835, <https://doi.org/10.1016/j.nanoen.2021.106835>.
- [44] P.Y. Feng, Z. Xia, B. Sun, X. Jing, H. Li, X. Tao, H.Y. Mi, Y. Liu, Enhancing the performance of fabric-based triboelectric nanogenerators by structural and chemical modification, *ACS Appl. Mater. Interfaces* 13 (2021) 16916–16927, <https://doi.org/10.1021/acsmi.1c02815>.
- [45] G. Min, Y. Xu, P. Cochran, N. Gadegaard, D.M. Mulvihill, R. Dahiya, Origin of the contact force-dependent response of triboelectric nanogenerators, *Nano Energy* 83 (2021), 105829, <https://doi.org/10.1016/j.nanoen.2021.105829>.
- [46] C. Kumar, D. Favier, T. Speck, V. Le Houérou, In situ investigation of adhesion mechanisms on complex microstructured biological surfaces, *Adv. Mater. Interfac.* 7 (2020) 57–62, <https://doi.org/10.1002/admi.202000969>.
- [47] Y. Xu, Y. Chen, A. Zhang, R.L. Jackson, B.C. Prorok, A new method for the measurement of real area of contact by the adhesive transfer of thin Au film, *Tribol. Lett.* 66 (2018) 1–20, <https://doi.org/10.1007/s11249-018-0982-5>.
- [48] R. Sahli, G. Pallares, C. Ducottet, I.E. Ben Ali, S. Al Akhrass, M. Guibert, J. Scheibert, Evolution of real contact area under shear and the value of static friction of soft materials, *Proc. Natl. Acad. Sci. U. S. A.* 115 (2018) 471–476, <https://doi.org/10.1073/pnas.1706434115>.
- [49] S.M.S. Rana, M.T. Rahman, S. Sharma, M. Salauddin, S.H. Yoon, C. Park, P. Maharjan, T. Bhatta, J.Y. Park, Cation functionalized nylon composite nanofibrous mat as a highly positive friction layer for robust, high output triboelectric nanogenerators and self-powered sensors, *Nano Energy* 88 (2021), 106300, <https://doi.org/10.1016/j.nanoen.2021.106300>.
- [50] S.M.S. Rana, M.T. Rahman, M. Salauddin, S. Sharma, P. Maharjan, T. Bhatta, H. Cho, C. Park, J.Y. Park, Electrospun PVDF-TrFE/MXene nanofiber mat-based triboelectric nanogenerator for smart home appliances, *ACS Appl. Mater. Interfaces* 13 (2021) 4955–4967, <https://doi.org/10.1021/acsmi.0c17512>.
- [51] G. Min, A. Pullanchiyodan, A.S. Dahiya, E.S. Hosseini, Y. Xu, D.M. Mulvihill, R. Dahiya, Ferroelectric-assisted high-performance triboelectric nanogenerators based on electrospun P(VDF-TrFE) composite nanofibers with barium titanate nanofillers, *Nano Energy* 90 (2021), 106600, <https://doi.org/10.1016/j.nanoen.2021.106600>.
- [52] D.-J. Sim, G.-J. Choi, S.-H. Sohn, I.-K. Park, Electronegative polyvinylidene fluoride/C60 composite nanofibers for performance enhancement of triboelectric nanogenerators, *J. Alloys Compd.* 898 (2022), 162805.
- [53] J. Xia, Z. Zheng, Y. Guo, Mechanically and electrically robust, electro-spun PVDF/PMMA blend films for durable triboelectric nanogenerators, *Compos. Part A Appl. Sci. Manuf.* (2022), 106914.
- [54] M.T. Rahman, S.M.S. Rana, M.A. Zahed, S. Lee, E.-S. Yoon, J.Y. Park, Metal-organic framework-derived nanoporous carbon incorporated nanofibers for high-performance triboelectric nanogenerators and self-powered sensors, *Nano Energy* (2022), 106921.
- [55] P. Tofel, K. Částková, D. Ríha, D. Sobola, N. Papež, J. Kaštyl, S. Talu, Z. Hadaš, Triboelectric response of electrospun stratified PVDF and PA structures, *Nanomaterials* 12 (2022) 349, 2022.
- [56] Y. Hao, J. Huang, S. Liao, D. Chen, Q. Wei, All-electrospun performance-enhanced triboelectric nanogenerator based on the charge-storage process, *J. Mater. Sci.* (2022) 1–12.
- [57] Z. Sha, C. Boyner, G. Li, Y. Yu, F.-M. Allieux, K. Kalantar-Zadeh, C.-H. Wang, J. Zhang, Electrospun liquid metal/PVDF-HFP nanofiber membranes with exceptional triboelectric performance, *Nano Energy* 92 (2022), 106713.

- [58] S. Bairagi, G. Khandelwal, X. Karagiorgis, S. Gokhool, C. Kumar, G. Min, D. M. Mulvihill, High-Performance Triboelectric Nanogenerators Based on Commercial Textiles : Electrospun Nylon 66 Nanofibers on Silk and PVDF on Polyester, 2022, <https://doi.org/10.1021/acsami.2c13092>.
- [59] A. Babu, I. Aazem, R. Walden, S. Bairagi, D.M. Mulvihill, S.C. Pillai, Electrospun nanofiber based TENGs for wearable electronics and self-powered sensing, Chem. Eng. J. 452 (2022), <https://doi.org/10.1016/j.cej.2022.139060>, 139060.
- [60] K. Dong, Y. Hu, J. Yang, S.W. Kim, W. Hu, Z.L. Wang, Smart textile triboelectric nanogenerators: current status and perspectives, MRS Bull. 46 (2021) 512-521, <https://doi.org/10.1557/s43577-021-00123-2>.